NACA

RESEARCH MEMORANDUM

DRAG AND HEAT TRANSFER ON A PARABOLIC BODY OF REVOLUTION (NACA RM-10) IN FREE FLIGHT TO MACH NUMBER 2 WITH BOTH CONSTANT AND VARYING REYNOLDS NUMBER AND HEATING EFFECTS ON TURBULENT SKIN FRICTION

By Joseph P. Maloney

Langley Aeronautical Laboratory
Langley Field, Va.

CLASSIFIED DOCUMENT

NATIONAL ADVISORY COMMITTEE
FOR AERONAUTICS

WASHINGTON
June 17, 1954

Classification cancelled (or changed to) Unclassified
By authority of: Nasa Tech Pub Announcement #79
By ..... (OFFICER AUTHORIZED)
13 Apr. 56
(GRADE OF OFFICER MAKING CHANGE)
6 Apr. 61
(DATE)

1F

NACA RM L54D06

[redacted]

NATIONAL ADVISORY COMMITTEE FOR AERONAUTICS

RESEARCH MEMORANDUM

DRAG AND HEAT TRANSFER ON A PARABOLIC BODY OF REVOLUTION (NACA RM-10) IN FREE FLIGHT TO MACH NUMBER 2 WITH BOTH CONSTANT AND VARYING REYNOLDS NUMBER AND HEATING EFFECTS ON TURBULENT SKIN FRICTION

By Joseph P. Maloney

SUMMARY

A flight test of a research model, designated NACA RM-10, was undertaken to obtain experimental drag and heat-transfer data under both constant and varying conditions of Reynolds number and heating effects. The model was a parabolic body of revolution with a fineness ratio of 12.2, stabilized by four 60° sweptback fins equally spaced around the base of the model. The data were obtained for Mach numbers from 1.35 to 2.01.

Average body turbulent skin-friction-drag coefficients have been determined when the heating effect on the skin friction was (a) constant and (b) varying. The measured coefficients agreed with Van Driest's theory for turbulent flow over a flat plate.

Temperature recovery factors were obtained from several skin-temperature measurements along the body. Local aerodynamic heat-transfer data, correlated on a Nusselt, Prandtl, and Reynolds number basis, were in good agreement with results from previous investigations on two NACA RM-10 models. The Reynolds numbers, based on axial distance from the nose station to the temperature-measurement stations, varied from 5.7×10^6 to 111.3×10^6.

Heat-transfer data, correlated on a Nusselt and Reynolds number basis which utilizes the boundary-layer thickness as the characteristic length, were in good agreement with a theory for turbulent boundary layers.

A preliminary attempt to verify experimentally Reynolds analogy by integrating the local heat-transfer data to obtain average skin-friction-drag coefficients yielded agreement within 8 percent of the measured average skin-friction-drag coefficients.

[redacted]

[redacted]

INTRODUCTION

As a continuation of the program of obtaining experimental data on drag and aerodynamic heat transfer on a parabolic body of revolution, designated the NACA RM-10, the National Advisory Committee for Aeronautics has flight tested a model at the Langley Pilotless Aircraft Research Station at Wallops Island, Va. The purposes of the flight test were (1) to obtain experimental turbulent average skin-friction-drag coefficients as a function of Mach number only, for a constant Reynolds number and a constant heating effect; (2) to obtain experimental average skin-friction drag, base drag, total drag, and aerodynamic heat-transfer data for a range of Reynolds number, Mach number, and heating; and (3) to obtain experimental verification of Reynolds' analogy, relating skin friction to heat transfer.

The Mach number range covered in fulfillment of purpose (1) was from 1.35 to 1.99 while Reynolds number per foot had a relatively small variation from 8.4×10^6 to 6.3×10^6. During the time of flight satisfying condition (2), the Mach number varied from 1.35 to 2.01, with a Reynolds number per foot range from 2.4×10^6 to 11.3×10^6. The investigation was conducted at zero angle of attack.

SYMBOLS

A	surface area, sq ft
C	specific heat of skin, Btu/(lb)(°F)
C_{D_b}	base-drag coefficient, based on body frontal area, dimensionless
C_{D_F}	average body skin-friction-drag coefficient, based on body frontal area, dimensionless
C_{D_T}	total drag coefficient, based on body frontal area, dimensionless
c_f	local skin-friction coefficient based on model surface area, dimensionless
C_F	average skin-friction coefficient based on model surface area, dimensionless
C_H	Stanton number, $\frac{h}{c_p \rho V}$, dimensionless

c_p	specific heat of air at constant pressure, Btu/(slug)($^\circ$F)
C_{P_b}	base-pressure coefficient, $\frac{P_b - P_\infty}{q_\infty}$, dimensionless
g	gravitational acceleration, 32.2 ft/sec^2
h	local heat-transfer coefficient, Btu/(sec)(ft)^2($^\circ$F)
J	mechanical equivalent of heat, 778 ft-lb/Btu
k	thermal conductivity of air, Btu/(sec)(ft)($^\circ$F)
l	axial length to measurement station, ft
M	Mach number, dimensionless
Nu	Nusselt number, $\frac{hl}{k}$, dimensionless
P	pressure, lb/sq ft
Pr	Prandtl number, $\frac{c_p\mu}{k}$, dimensionless
q	dynamic pressure, lb/sq ft
Q	quantity of heat, Btu
R	Reynolds number, $\frac{Vl\rho}{\mu}$, dimensionless
R.F.	recovery factor, $\frac{T_{aw} - T_\delta}{T_o - T_\delta}$, dimensionless
t	time, sec
T_∞	free-stream static temperature, $^\circ$F absolute
T_δ	local static temperature, just outside the boundary layer, $^\circ$F absolute
T_{aw}	adiabatic wall temperature, $^\circ$F absolute

[redacted]

T_w	skin temperature, °F absolute
T_o	stagnation temperature, °F absolute
u	velocity in the boundary layer, ft/sec
V	velocity, ft/sec
ρ	density, slugs/cu ft
w	specific weight of model skin, lb/cu ft
δ	boundary-layer thickness, ft
τ	thickness of model skin, ft
μ	viscosity of air, slugs/ft-sec

Subscripts:

∞	free-stream conditions
δ	conditions just outside boundary layer
b	conditions at base of model
l	conditions at outer edge of sublayer
j	conditions in jet exhaust

MODEL, INSTRUMENTATION, AND TEST

Model

The model used in the investigation is shown in figure 1, together with the basic body equation. A photograph of the model on the launcher is shown in figure 2.

The model was a parabolic body of revolution, designated the NACA RM-10, having a fineness ratio of 12.2. Four 60° sweptback untapered stabilizing fins, having a 10-percent-thick circular-arc profile perpendicular to the leading edge, were equally spaced around the stern. The maximum diameter of the body was 12 inches, giving a reference frontal area for drag coefficients of 0.785 square foot. The length of the body was 146.5 inches. The body, forward of the 129-inch station, was made of

spun magnesium alloy. The tail section was cast magnesium, to which were welded cast magnesium fins.

The sustainer rocket motor adapted for this test was a JATO, 14-DS-1000, which made it possible to accelerate the model through the Mach number range with a relatively small change in Reynolds number. To insure adequate model stability, the center of gravity of the internal JATO rocket motor was located at station 93, which necessitated the addition of a low-pressure tailpipe to the exhaust nozzle, extending rearward to the base of the model. The tailpipe was cylindrical, so that the exhaust gases exited with negligible transverse velocity. The exit Mach number of the propulsive jet was approximately 3.3.

Instrumentation

Skin temperatures were measured throughout the flight by means of resistance wire pickups installed at the 29-, 73-, and 120-inch stations. This measurement technique is fully described in reference 1.

Base pressure was measured in the annulus between the tailpipe and the skin, 1.87 inches from the model center line, on a radial line from the model center line to a fin as shown in figure 3. The annular area was sealed from the forward portion of the body to prevent internal air flow. A jet exit pressure was measured 3/4 inch from the end of the rocket exhaust nozzle. During coasting flight, this provided an additional measurement of base drag.

A boundary-layer total-pressure rake, shown in figure 4, was located at station 124 to provide data for calculating the average skin-friction-drag coefficient.

Longitudinal acceleration was measured by thrust and drag accelerometers. Temperatures, pressures, and accelerations were continuously telemetered to ground receiving stations throughout the flight.

Atmospheric data were obtained from radiosonde observations made at the time of the flight. Velocity and model position were measured by Doppler velocity radar and SCR-584 radar, respectively. Velocity for the heat-transfer data was obtained after the range of Doppler radar was exceeded (26.8 seconds) by integrating the drag-accelerometer measurements.

Test

The model was launched from a zero-length launcher at an elevation angle of 60° by means of a booster consisting of two 6.25-inch ABL Deacon rocket motors (see fig. 2), which burned for 3.2 seconds, accelerating

the model to Mach number 1.59. After the booster thrust was expended, the booster drag-separated from the model. The model then coasted for 3.3 seconds until the 14-DS-1000 JATO sustainer rocket motor ignited. Approximately 14 seconds of accelerating flight followed and at the time of sustainer burnout the peak Mach number of 2.01 was attained. The JATO, 14-DS-1000 sustainer rocket motor enabled the model to accelerate through the Mach number range with a relatively small change in Reynolds number, since the model was increasing in altitude. During the remainder of the flight after 20.5 seconds, the model decelerated. The variations with time of Mach number and Reynolds number per foot are shown in figure 5. The time histories of the stagnation temperature and the skin temperature for a typical measurement station are shown in figure 6.

RESULTS AND DISCUSSION

Skin Friction

Average body skin-friction-drag coefficients were determined from boundary-layer total-pressure-rake measurements at the 124-inch station using the boundary-layer momentum procedure as developed in reference 2. The temperature distribution through the boundary layer was calculated, using the theory of reference 3. Figure 7 presents the time history of the average skin-friction coefficient. The measured data, indicated by the circled points, cover a range of Reynolds numbers, Mach numbers, and heating conditions. The comparison of the measured data with the solid line of figure 7, representing Van Driest's theory for turbulent flow over a flat plate (ref. 4), showed excellent agreement, both in magnitude and trend. The presence of a temperature gradient along the surface of the body was accounted for in determining the theoretical values of average skin-friction coefficients by using the surface temperature at the average area station as the model's characteristic temperature. The average area station is the location where the model surface area forward of this station is equal to the surface area rearward of the station, back to the boundary-layer measurement station. The data points can be assumed to be the average skin-friction coefficient for turbulent flow on the NACA RM-10 body, since turbulent flow was present over practically all of the surface area of the model.

Average skin-friction coefficients for insulated surfaces are known to be functions of Reynolds number and Mach number, according to theories developed in references 5, 6, and 7. When the surface on which the skin friction is acting is not insulated, that is, the wall temperature is not equal to the adiabatic wall temperature, an additional effect, namely heating, influences the skin friction. The variation of this heating effect, as expressed by the parameter $\frac{T_{aw} - T_w}{T_{aw} - T_\delta}$ developed in the appendix,

is shown in figure 8 for the three skin-temperature measurement stations. At 3.5 seconds, the heating parameter was 0.75, indicating that the model's surface temperature had negotiated only 25 percent of the adiabatic temperature rise. The parameter decreased continuously until 6.5 seconds when the sustainer rocket motor ignited, which accelerated the model for approximately 14 seconds. During this accelerating flight, the heating parameter remained essentially constant for all three temperature stations. After burnout of the sustainer rocket motor, approximately 21 seconds, the heating parameter resumed its decrease with time. Equilibrium temperatures occurred at approximately 23 seconds, after which the wall temperature was hotter than the adiabatic wall temperature.

Consideration of the effects of Reynolds number and Mach number on the average skin-friction coefficient was undertaken during the flight time between 6.5 and 21 seconds, when the heating effect upon skin friction was a constant. For this interval, the Mach number increased from 1.35 to 1.99 while Reynolds number per foot decreased from 8.4×10^6 to 6.3×10^6. Figure 9 presents the measured average skin-friction data for this heating condition, plotted against Mach number. Van Driest's turbulent flat-plate theory for the flight conditions encountered is shown by the solid line. The temperature parameter for the average area station for this time was 0.24. During this time interval, a small change in Reynolds number occurred, rendering the measured data of figure 9 as a function of both Reynolds number and Mach number. The effect on skin friction of this variation in Reynolds number can be shown by the dashed line of figure 9 which is the theoretical line (ref. 4) for both constant heating and constant Reynolds number. The Reynolds number based on length to the measurement station used in obtaining this curve was 8.7×10^7, which occurred at the onset of the constant heating period. This curve indicates that the change in Reynolds number caused an increase of 3 percent in skin-friction coefficient. The increase in Mach number from 1.35 to 1.99 resulted in a reduction of 9 percent in average skin-friction coefficient.

During the portions of the flight exclusive of the 6.5- to 21-second portion, large variations in heating effects, together with the variation in Mach and Reynolds numbers, prevented the isolation of the influence of any one of these parameters on skin friction. However, as noted in the discussion of figure 7, the measured values of average skin-friction coefficients for this portion, also agreed well with Van Driest's theory. The skin friction accounts for approximately one-third of the total drag of the model as will be shown subsequently.

[redacted]

Recovery Factor

The boundary-layer recovery factor is defined as

$$R.F. = \frac{T_{aw} - T_{\delta}}{T_o - T_{\delta}} \tag{1}$$

The temperature T_{δ} was obtained throughout the flight by correcting the free-stream static temperature for the pressure distribution along the body. Stream static and stagnation temperatures were obtained from trajectory and radiosonde data. Stagnation temperature reached a maximum at the peak Mach number, and thereafter decreased as the model decelerated. The model skin temperature reached a maximum during the coasting flight following the burnout of the sustainer rocket motor. When the radiation and conduction along the surface are negligible, as in the model tested, the maximum surface temperature is equal to the adiabatic wall temperature. Recovery factors therefore were determined at the peak of the skin-temperature curve and are plotted in figure 10 against longitudinal distance from the nose station. The measured recovery factors are in good agreement with the theoretical turbulent value of $Pr^{1/3}$ obtained from reference 8.

Heat Transfer

The aerodynamic heat transfer was determined from temperatures measured during the transient heating of the model. When radiation from the model and conduction along the surface are negligible, the heat transferred to the model by convection can be equated to the heat accumulated by the skin:

$$\frac{dQ}{dt} = hA\left(T_{aw} - T_w\right) = w_T AC \frac{dT_w}{dt} \tag{2}$$

Equation (2) can be solved for the convective heat-transfer coefficient:

$$h = \frac{w_T C \frac{dT_w}{dt}}{T_{aw} - T_w} \tag{3}$$

Wall properties of density, thickness, and specific heat were known quantities, while the skin temperature and its time rate of change were measured during the flight test. The adiabatic-wall-temperature variation with time was calculated from equation (1) by assuming that the recovery factor was constant throughout the flight.

Figure 11 presents the heat transfer for the three temperature measurement stations (29, 73, and 120), correlated on a Nusselt, Prandtl, and Reynolds number basis. Flow properties are based on conditions just outside the boundary layer, while the Reynolds number is based on the length to the measuring station. The data points are in good agreement with the turbulent relation from reference 9, $NuPr^{-1/3} = 0.0296Re^{0.8}$ The data had an average scatter of approximately 12 percent around the line representing the equation. Results obtained from this flight test and the previous results of reference 9 indicate that the equation could be used to predict surface temperatures with good accuracy for supersonic speeds up to $M = 2.8$.

Heat transfer to bodies of high fineness ratio, for which the local Reynolds number is approximately equal to the free-stream Reynolds number, can be correlated on free-stream conditions without incurring any loss in accuracy. This would facilitate estimations of skin temperature on bodies and surfaces by eliminating the necessity of calculating local flow conditions along the body. Figure 12 presents the heat transfer from the current flight test, correlated on a Nusselt, Prandtl, and Reynolds number basis and using free-stream flow conditions. The average scatter of the data about the line representing the equation $NuPr^{-1/3} = 0.0296R^{0.8}$ is 13 percent, which is comparable to results based on local flow conditions.

Heat-transfer data from the 120-inch station are correlated in figure 13 according to Donaldson's theory (ref. 10), which utilizes the boundary-layer thickness as the significant length. The data are correlated as Reynolds number plotted against Nusselt number multiplied by a factor F which embodies the Mach number and heating effects. The boundary-layer thickness was determined from the boundary-layer pressure-rake measurements. Comparison of the data with the equation $FNu = 0.0225R^{0.75}$ shows an average deviation of approximately 8 percent The equation was developed for a 1/7-power velocity profile whereas the measured profile was approximately to the 1/8 power. Lack of measured boundary-layer thicknesses at stations 29 and 73 prevented their correlation on this basis.

Figure 14 presents the heat-transfer data from figure 11 transposed to a Stanton number and Reynolds number basis. The line represents the equation $C_H = 0.0365R^{-0.2}$ which is equivalent to the curve from

[redacted]

figure 11, assuming the Prandtl number to be equal to 0.73. Flow properties are based on local conditions just outside the boundary layer. The scatter of the data was partly attributed to the range of Mach number and heating conditions covered.

Reynolds' analogy of heat transfer and skin friction is expressed in reference 11 as

$$C_H = \frac{c_f}{2} \tag{4}$$

However, this is based on a Prandtl number of unity. Rubesin (ref. 12) modified Reynolds analogy to

$$C_H = \left(\frac{1 + \frac{u_1}{u_\infty}}{R.F. + Pr \frac{u_1}{u_\infty}} \right) \frac{c_f}{2} \tag{5}$$

and showed that, for a Prandtl number of 0.72, the term in parentheses can be assumed to be 1.20 within 2-percent accuracy for Mach numbers up to 5. From the measured Stanton numbers C_H for stations 29, 73, and 120, local skin-friction coefficients were determined by equation (5). Forward of station 29 the variation of C_H with distance was estimated using the trends predicted by reference 4. Average skin-friction coefficients therefore could be obtained by integrating the heat-transfer parameter C_H with respect to the body surface area. Figure 15 presents a comparison of the average skin-friction coefficients, obtained by integrating the heat-transfer data, with the measured average skin-friction coefficients reproduced from figure 7. The solid line is the theory for turbulent average skin-friction coefficient from reference 4. The values from the integrated heat transfer agree within 8 percent of the measured C_F, which, when considering the meager number of heat-transfer stations, can be considered remarkably good agreement.

Total Drag

Total drag coefficients for the two coasting portions of the flight were reduced from Doppler radar data and are shown in figure 16 plotted against Mach number. A reduction in coefficient occurs with increasing Mach number during each portion. A Mach number range from 1.55 to 1.36 was covered during the first coast. The second coast Mach number decreased from 1.99 to 1.64, at which time the range of the Doppler radar

was exceeded. The magnitude of the total drag coefficients is in good agreement with those reported in reference 13.

The skin-friction-drag data for the coasting flight are shown in figure 16 as a drag coefficient C_{D_F}, based on body frontal area. The body skin-friction drag accounts for approximately one-third of the total drag of the model.

Base Drag

Base-drag coefficients, determined by measured base pressure, are shown by the bottom curve of figure 16. Both coasting portions of the flight are represented by the curve since the data from each portion were in good agreement. The corresponding base-pressure coefficients are shown in figure 17(a) by the curve labeled "Power off." Results from a previous investigation of base-pressure coefficients (ref. 13) are shown by the dashed line in figure 17(a) to be approximately 30 percent less at the lower Mach numbers. During the coasting portion of the present flight test, both the jet-pressure orifice and the base-pressure orifice measured the base pressure. The values of C_{p_b} from the two measurements agreed within 0.01, indicating that the disagreement with reference 13 was not a result of a faulty pressure measurement. A possible reason for the disagreement lies in the difference in the location of the pressure orifice. In reference 13, the pressure orifice measured the average pressure acting on an annulus extending from the nozzle lip to the model skin, a distance of 0.511 inch. The midpoint of this area would be 3.38 inches from the model center line. Base pressures reported herein were measured at 1.31 and 1.87 inches from the model center line as shown in figure 3. Should any pressure gradients occur over the base, the largest gradient would exist near the model surface. Therefore, a measurement which includes the effect of this edge gradient, as in reference 13, would read a higher value of base pressure, thereby a lower base drag. Conversely, a measurement close to the model center line, as on this flight model, would read a lower pressure, and a higher base drag.

Base pressure in the annulus around the nozzle exit and jet-exit pressure were measured during the period of the sustainer rocket motor firing and are presented in figures 17(a) and 17(b), respectively, as base-pressure coefficients and jet-exit pressure ratio plotted against the free-stream Mach number. The sustainer rocket motor ignited at 6.5 seconds of flight time, and accelerated the model from a Mach number of 1.35 to 2.01. Comparison of the power-on and power-off pressure coefficients shows the effect of the exhaust jet. Ignition of the rocket motor caused a sudden decrease in base-pressure and pressure coefficient, which, compared to power-off values, remained lower throughout the thrusting period of the flight. The variation of the ratio of jet-exit

pressure to free-stream pressure is shown in figure 17(b). The jet-pressure ratio, being greater than 1, indicates that the exhaust jet is underexpanded. The increase in jet-pressure ratio shown in the curve was due to the decrease of the free-stream static pressure since the altitude of the model was increasing. The model body had a 4.8° boattail angle at the base, while the Mach number of the exhaust gas was approximately 3.3. For the test conditions, the base-pressure coefficient with power on increased with increasing Mach number and jet-exit pressure ratio. This trend is in agreement with current investigations being conducted on boattailed bodies at supersonic speeds.

CONCLUDING REMARKS

The flight test has yielded experimental data for three phases of the investigation of aerodynamic characteristics of a parabolic body of revolution: (1) drag coefficients, (2) turbulent heat-transfer coefficients, and (3) Reynolds' analogy relating measured heat transfer to measured skin friction. The following remarks are based on results of the present investigation.

The average skin-friction coefficients for turbulent flow have been measured on the NACA RM-10 body over a Mach number range of 1.35 to 2.01 when the heating effect on skin friction was (a) constant and (b) varying. The Reynolds number remained approximately constant during the flight time, satisfying condition (a) so that the change in skin-friction coefficient was essentially a function of Mach number only. Skin-friction data for condition (b) covered a Reynolds number per foot range from 2.4×10^6 to 11.3×10^6. The coefficients were in good agreement with Van Driest's theory for average skin-friction coefficients on a flat plate.

Temperature recovery factors, which were determined from skin temperatures measured at three locations on the model, agreed well with the theoretical turbulent value of Prandtl number to the one-third power. Skin-temperature measurements on the model were reduced to heat-transfer data and correlated on a Nusselt, Prandtl, and Reynolds number basis. Good agreement of the data with the equation $NuPr^{-1/3} = 0.0296R^{0.8}$ was obtained with the air properties based on both free-stream conditions and local flow conditions just outside the boundary layer.

The heat-transfer data for the 120-inch station were correlated on Donaldson's basis, with an average agreement within 8 percent of the theory for a 1/7-power velocity profile.

In order to experimentally verify Reynolds' analogy between skin friction and heat transfer, complete axial distribution of heat-transfer

data was required which, when integrated with respect to the surface area over which it is acting, can be compared to the measured average skin friction. The integration of the faired heat transfer from three skin-temperature stations was found to yield average skin-friction coefficients which compared within 8 percent of the measured values. Although the meagerness of available temperature measurements prevented a conclusive experimental verification of the relation between heat transfer and skin friction, the results indicate preliminary proof of Reynolds' analogy.

Total drag and base-drag coefficients were determined during the coasting portions of the flight. Measured base-drag coefficients based on body frontal area varied from 0.044 to 0.057 as the velocity decreased from a Mach number of 1.98 to 1.35. During the accelerating portion of the flight, the presence of the jet exhausting from the sustainer rocket motor caused a reduction in the base-pressure coefficient throughout the Mach number range.

Langley Aeronautical Laboratory,
National Advisory Committee for Aeronautics,
Langley Field, Va., March 23, 1954.

[redacted]

APPENDIX

SURFACE HEATING CONDITIONS

The influence of the surface heating condition on skin-friction coefficients for noninsulated surfaces has been expressed by Van Driest (ref. 4) as a ratio of the skin temperature to the local free-stream temperature $\frac{T_w}{T_\delta}$. However, a constant value of $\frac{T_w}{T_\delta}$ does not indicate a constant heating condition as can be seen from the fact that $\frac{T_w}{T_\delta}$ for an insulated plate varies with the Mach number. The temperature distribution through the boundary layer can be expressed from reference 3 as

$$T = T_\delta - (T_{aw} - T_w)\left(1 - \frac{u}{V_\delta}\right) + \frac{R.F.(V_\delta^2 - u^2)}{2JgC_p} \qquad (A1)$$

Since $T_{aw} = T_\delta + R.F.\left(\frac{V_\delta^2}{2JgC_p}\right)$, equation (A1) can be arranged to yield

$$\frac{T - T_\delta}{T_{aw} - T_\delta} = \left(1 - \frac{u^2}{V_\delta^2}\right) - \frac{T_{aw} - T_w}{T_{aw} - T_\delta}\left(1 - \frac{u}{V_\delta}\right) \qquad (A2)$$

which expresses the temperature distribution in the boundary layer as a function of the velocity ratio and $\frac{T_{aw} - T_w}{T_{aw} - T_\delta}$. Therefore, for a given velocity profile, the nondimensional temperature profile would be determined by the ratio $\frac{T_{aw} - T_w}{T_{aw} - T_\delta}$. This means that a constant value of $\frac{T_{aw} - T_w}{T_{aw} - T_\delta}$ will yield geometrically similar temperature distributions.

[redacted]

A ratio $\frac{T_{aw} - T_w}{T_{aw} - T_\delta}$ of 1.0 would exist for a wall at free-stream temperature, while a ratio of zero indicates an insulated plate. A constant ratio would correspond to a constant proportion of the adiabatic temperature rise, regardless of Mach number. For a recovery factor of 0.90, the following values would result for two particular Mach numbers:

$\frac{T_{aw} - T_w}{T_{aw} - T_\delta}$	$\frac{T_w}{T_\delta}$ for M = 2	$\frac{T_w}{T_\delta}$ for M = 4
1.0	1	1
.5	1.36	2.44
0	1.72	3.88

In order to illustrate the significance of the ratio $\frac{T_{aw} - T_w}{T_{aw} - T_\delta}$, consider the temperature ratio of 0.5 from the above table. From the preceding discussion, the significance of the value is that the wall temperature has attained 50 percent of the temperature rise available between the stream static temperature and the adiabatic wall temperature. From the table, at a Mach number of 2.0, the ratio of the wall temperature to the stream static temperature was 1.36 which is 50 percent of the rise to the adiabatic condition of 1.72. Similarly at Mach number of 4.0, the ratio of $\frac{T_w}{T_\delta}$ would be 2.44, or 50 percent of the rise to adiabatic conditions. This quality of expressing the proportion of the temperature rise negotiated by the wall, together with its effect in determining the shape of the temperature profile through the boundary layer, justified the selection of the parameter $\frac{T_{aw} - T_w}{T_{aw} - T_\delta}$ as being indicative of the heating effect on the friction drag of the model.

[redacted]

REFERENCES

1. Fricke, Clifford L., and Smith, Francis B.: Skin-Temperature Telemeter for Determining Boundary-Layer Heat-Transfer Coefficients. NACA RM L50J17, 1951.

2. Rumsey, Charles B., and Loposer, J. Dan: Average Skin-Friction Coefficients From Boundary-Layer Measurements in Flight on a Parabolic Body of Revolution (NACA RM-10) at Supersonic Speeds and at Large Reynolds Numbers. NACA RM L51B12, 1951.

3. Crocco, Luigi: Transmission of Heat From a Flat Plate to a Fluid Flowing at a High Velocity. NACA TM 690, 1932.

4. Van Driest, E. R.: The Turbulent Boundary Layer for Compressible Fluids on a Flat Plate With Heat Transfer. Rep. No. AL-997, North American Aviation, Inc., Jan. 27, 1950.

5. Von Kármán, Th.: The Problem of Resistance in Compressible Fluids. Att: del V Convegno della Fondazione Alessandro Volta, R. Accad. d' Italia, vol. XIV, 1936, pp. 5-59.

6. Frankl, F., and Voishel, V.: Turbulent Friction in the Boundary Layer of a Flat Plate in a Two-Dimensional Compressible Flow at High Speeds. NACA TM 1053, 1943.

7. Wilson, Robert E.: Turbulent Boundary-Layer Characteristics at Supersonic Speeds - Theory and Experiment. Jour. Aero. Sci., vol. 17, no. 9, Sept. 1950, pp. 585-594.

8. Squire, H. B.: Heat Transfer Calculations for Aerofoils. R. & M. No. 1986, British A.R.C., 1946.

9. Chauvin, Leo T., and DeMoraes, Carlos A.: Correlation of Supersonic Convective Heat-Transfer Coefficients From Measurements of the Skin Temperature of a Parabolic Body of Revolution (NACA RM-10). NACA RM L51A18, 1951.

10. Donaldson, Coleman duP.: Heat Transfer and Skin Friction for Turbulent Boundary Layers on Heated or Cooled Surfaces at High Speeds. NACA RM L52H04, 1952.

11. Jakob, Max: Heat Transfer. Vol. I. John Wiley & Sons, Inc., 1949.

12. Rubesin, Morris W.: A Modified Reynolds Analogy for the Compressible Turbulent Boundary Layer on a Flat Plate. NACA TN 2917, 1953.

13. Jackson, H. Herbert, Rumsey, Charles B., and Chauvin, Leo T.: Flight Measurements of Drag and Base Pressure of a Fin-Stabilized Parabolic Body of Revolution (NACA RM-10) at Different Reynolds Numbers and at Mach Numbers From 0.9 to 3.3. NACA RM L50G24, 1950.

[redacted]

[redacted]

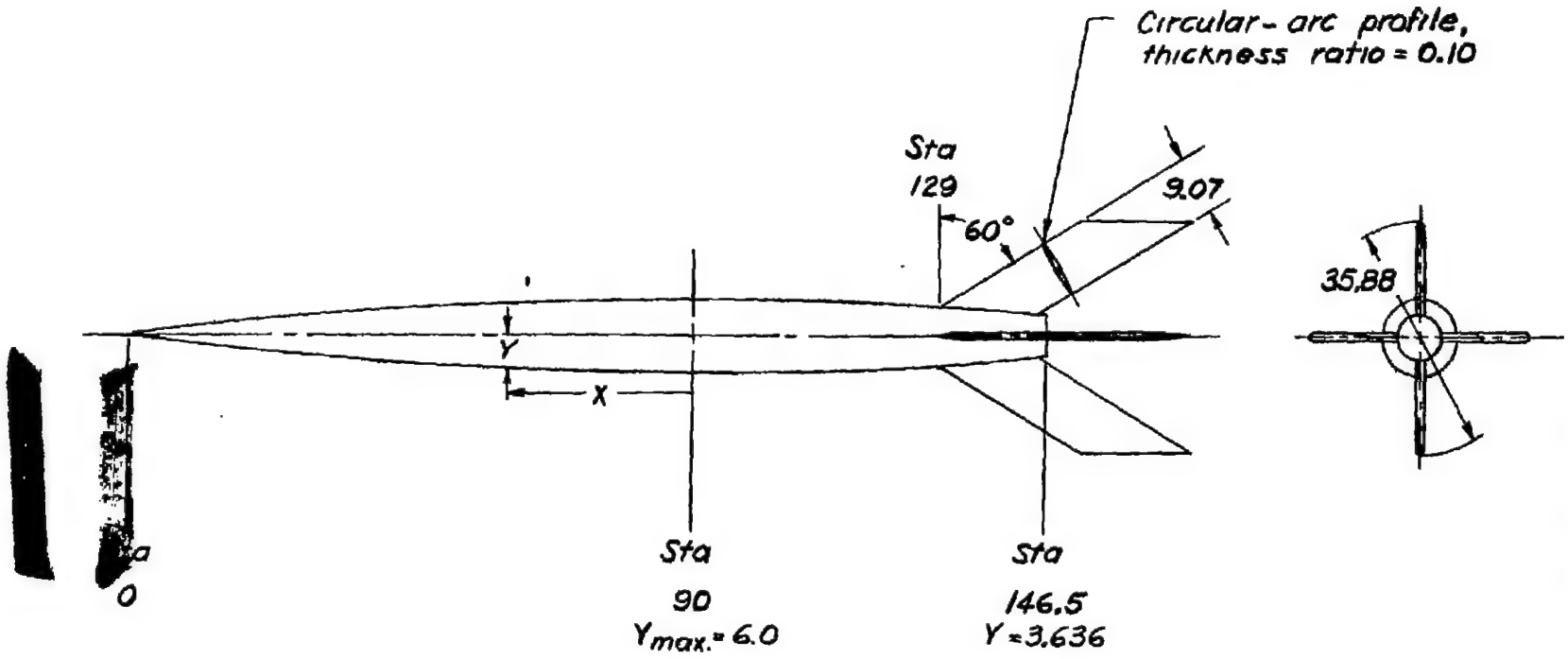

Body profile equation:

$$Y = 6.000 - 0.0007407X^2$$

Station number denotes axial distance from nose in inches.

Figure 1.- General configuration and body equation of the NACA RM-10. Dimensions are in inches.

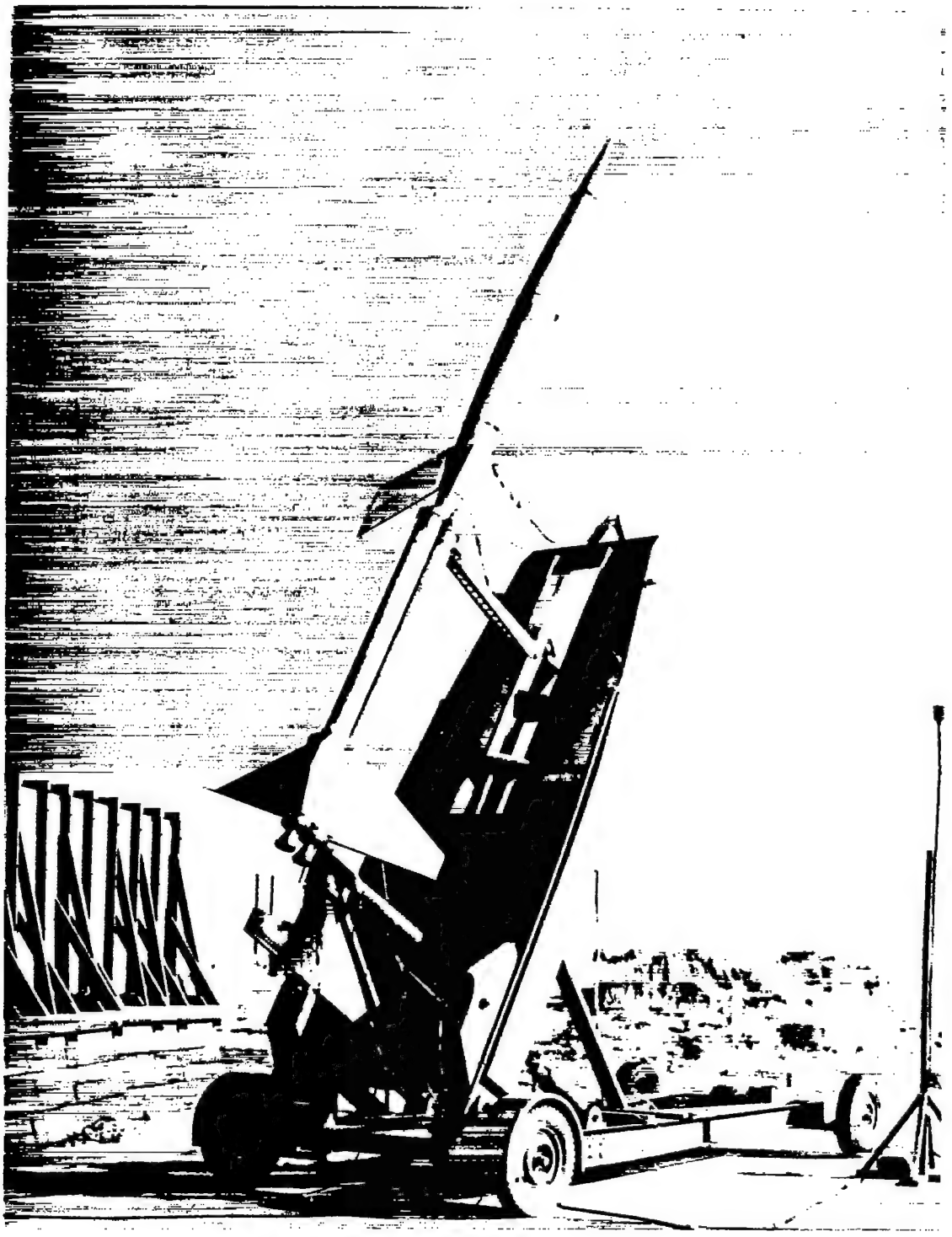

L-79056

Figure 2.- Photograph of flight model on the launcher.

[redacted]

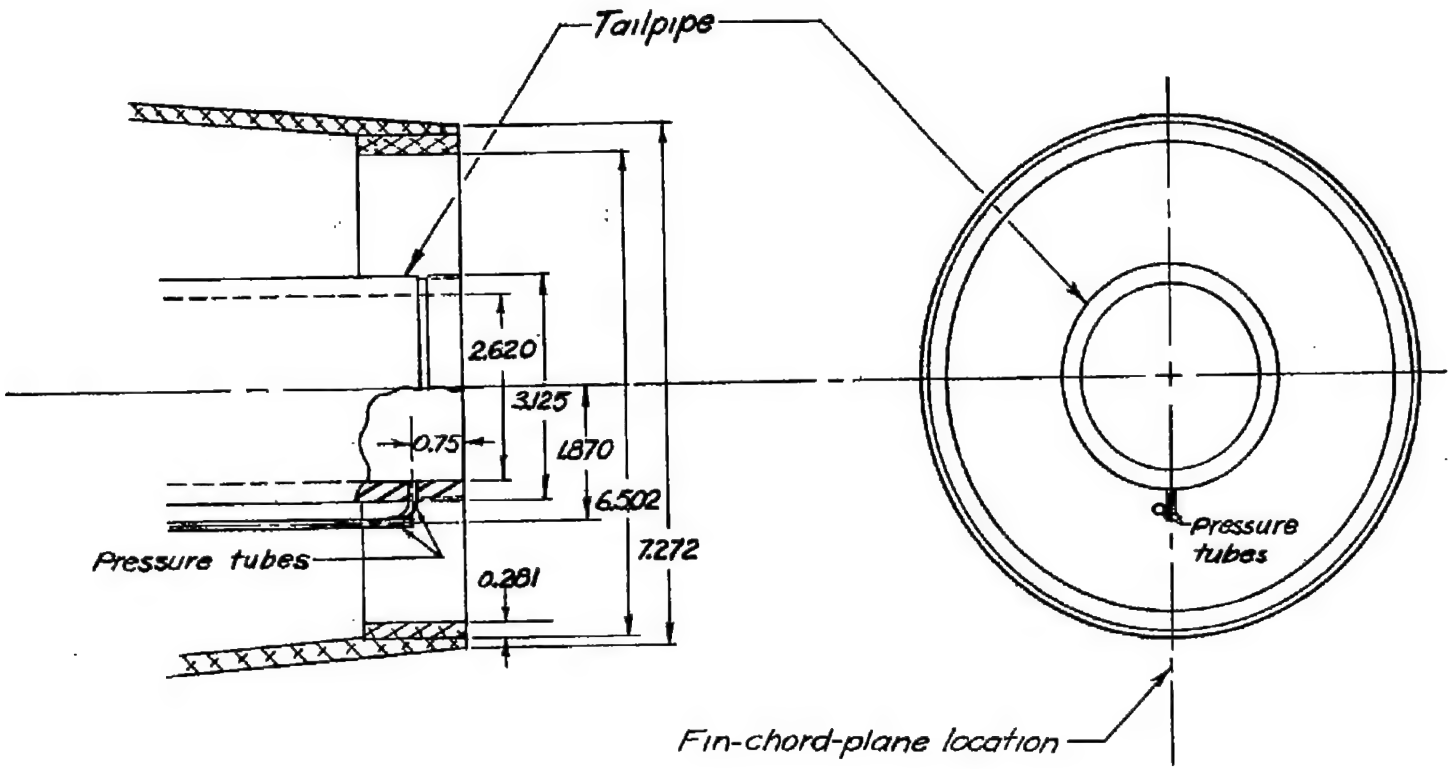

Figure 3.- Base configuration of model, showing location of base- and jet-exit-pressure tubes.

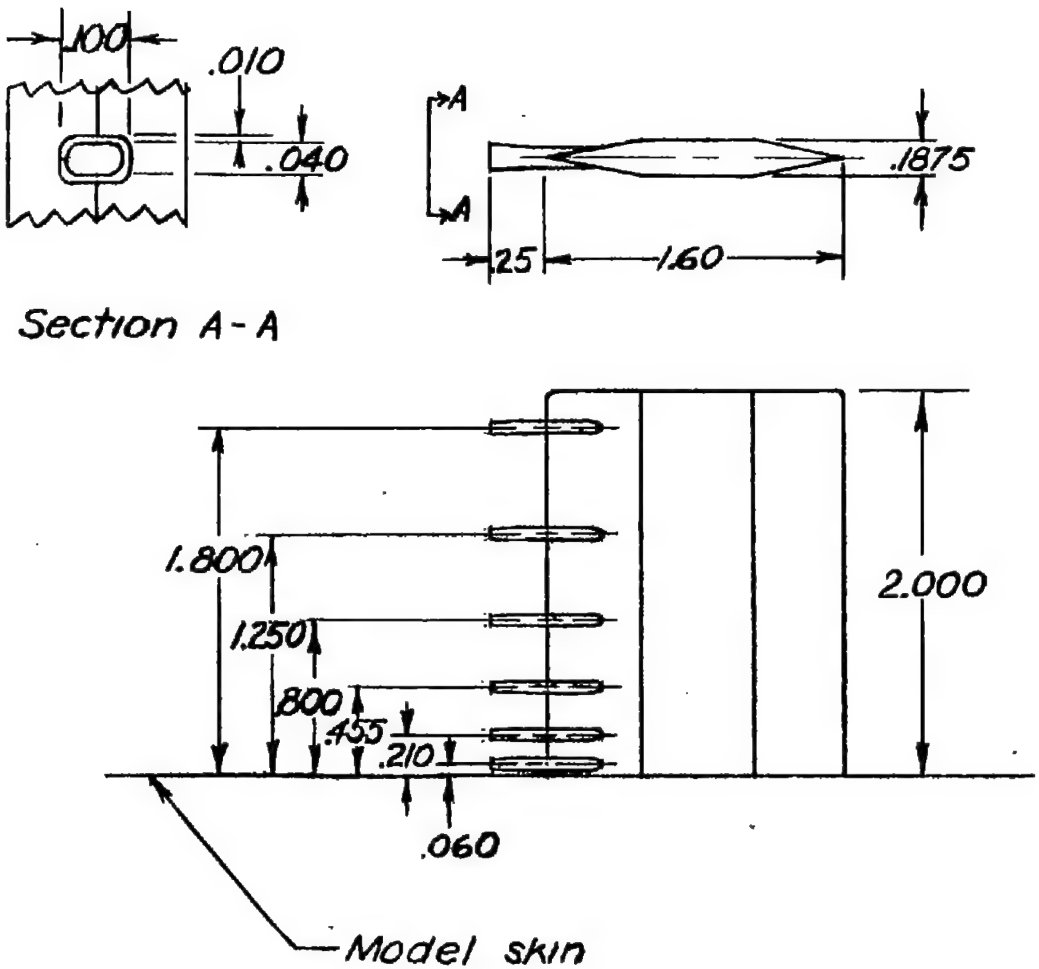

Figure 4.- General configuration of boundary-layer total-pressure rake. All dimensions are in inches.

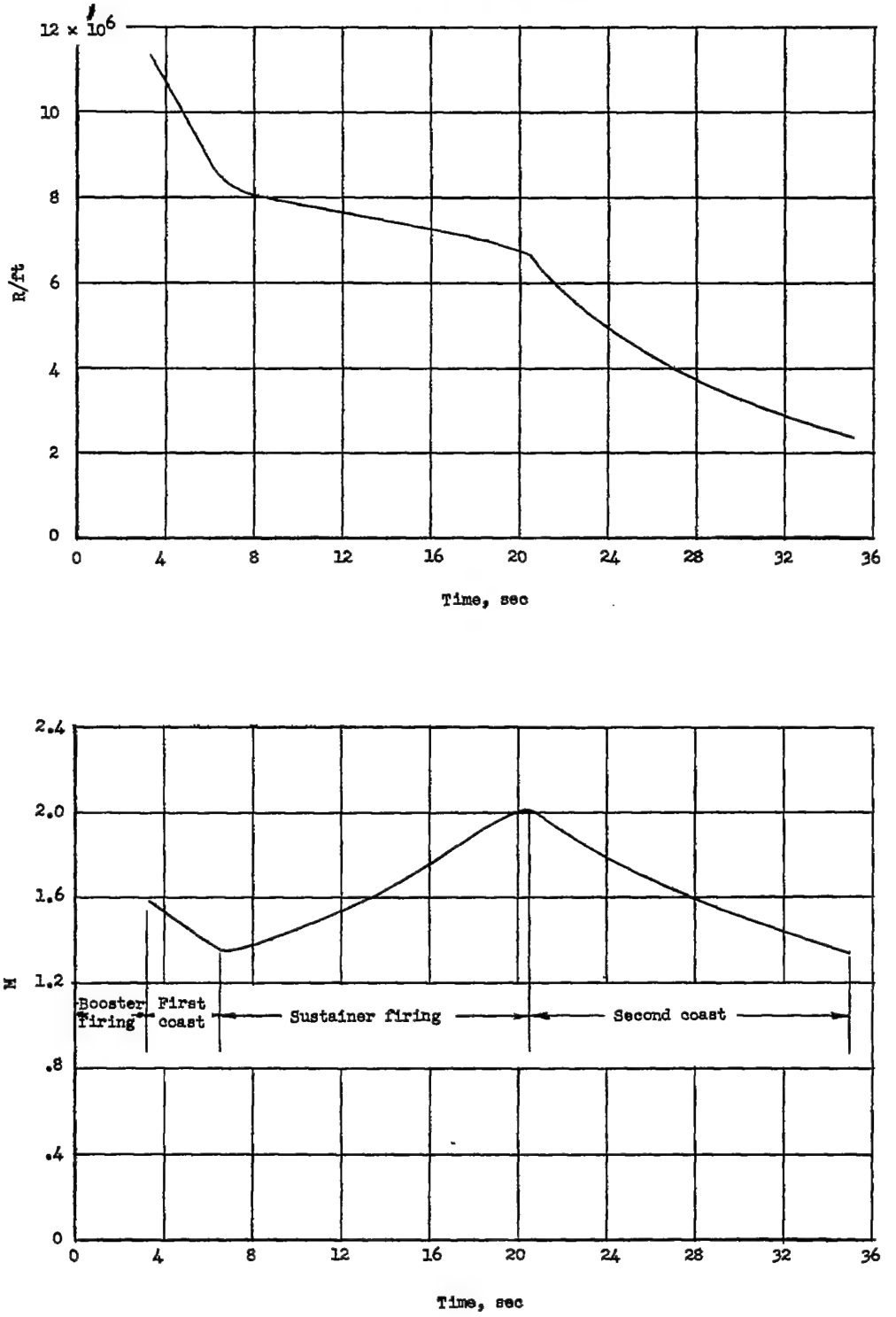

Figure 5.- Time history of Reynolds number and Mach number.

[redacted]

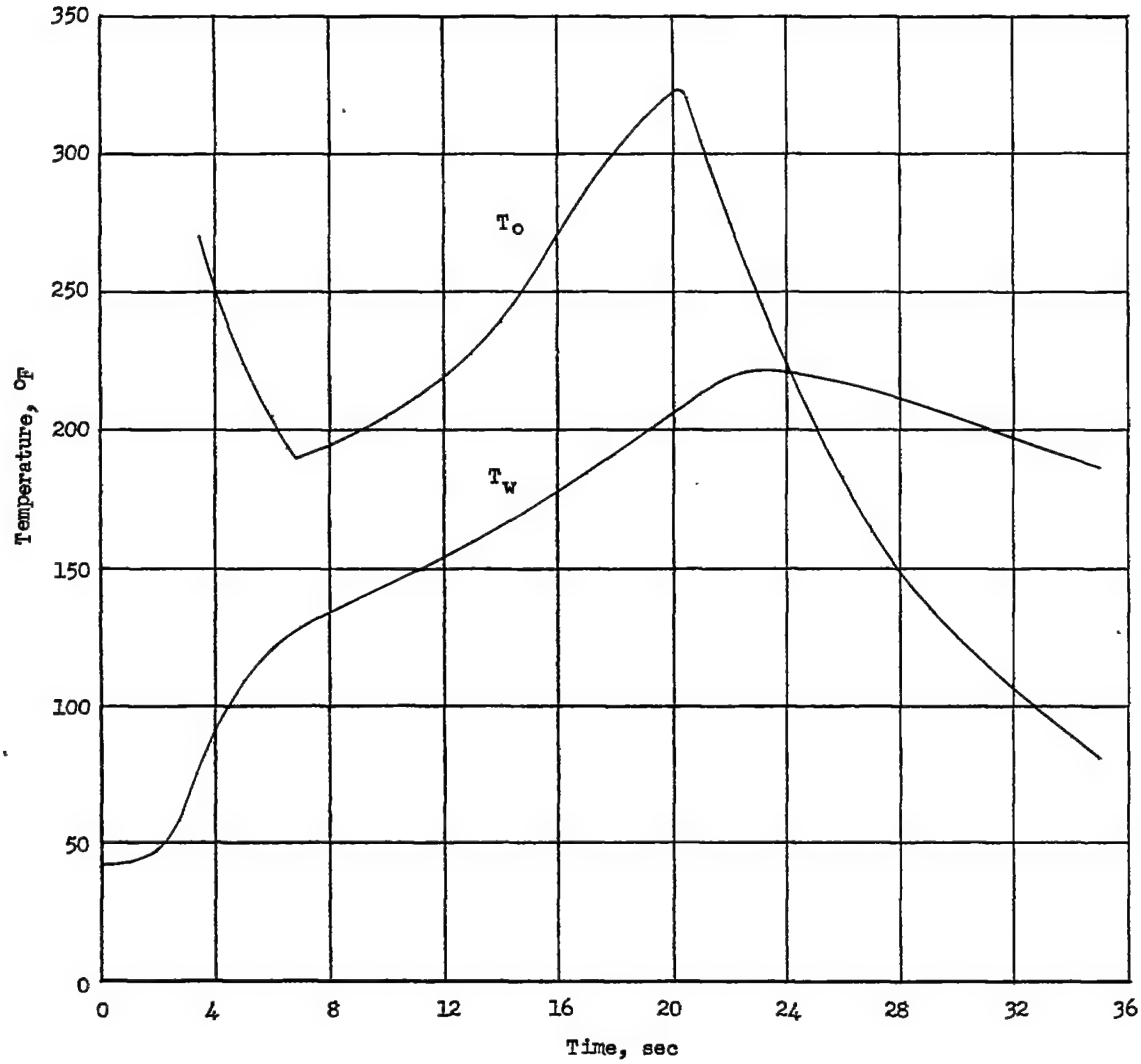

Figure 6.- Time history of stagnation temperature and skin temperature for a typical measurement station.

[redacted]

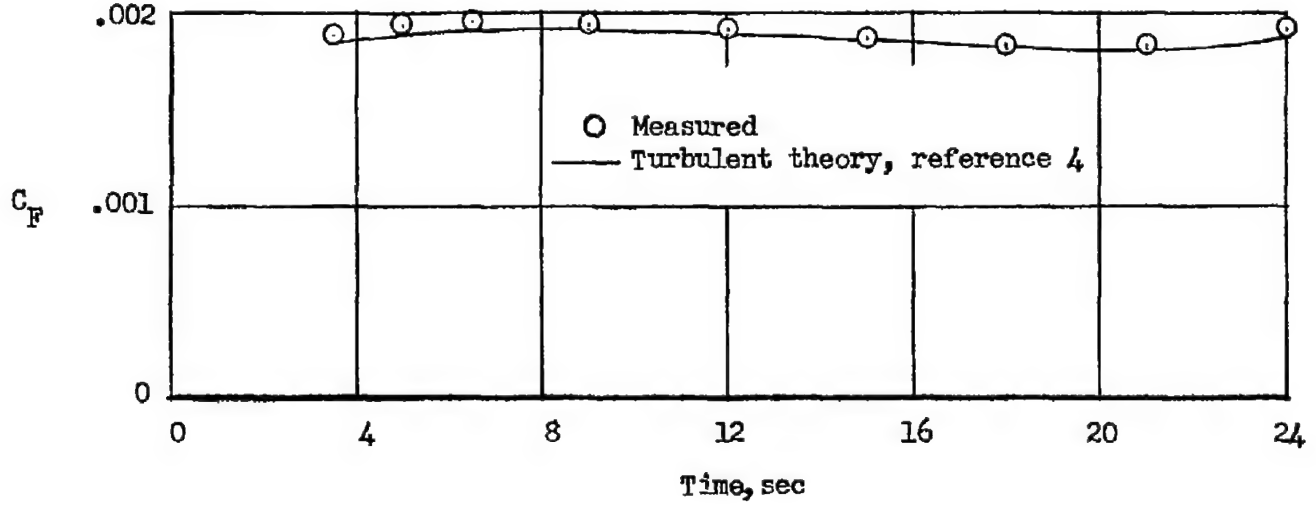

Figure 7.- Time history of measured and theoretical average skin-friction coefficients.

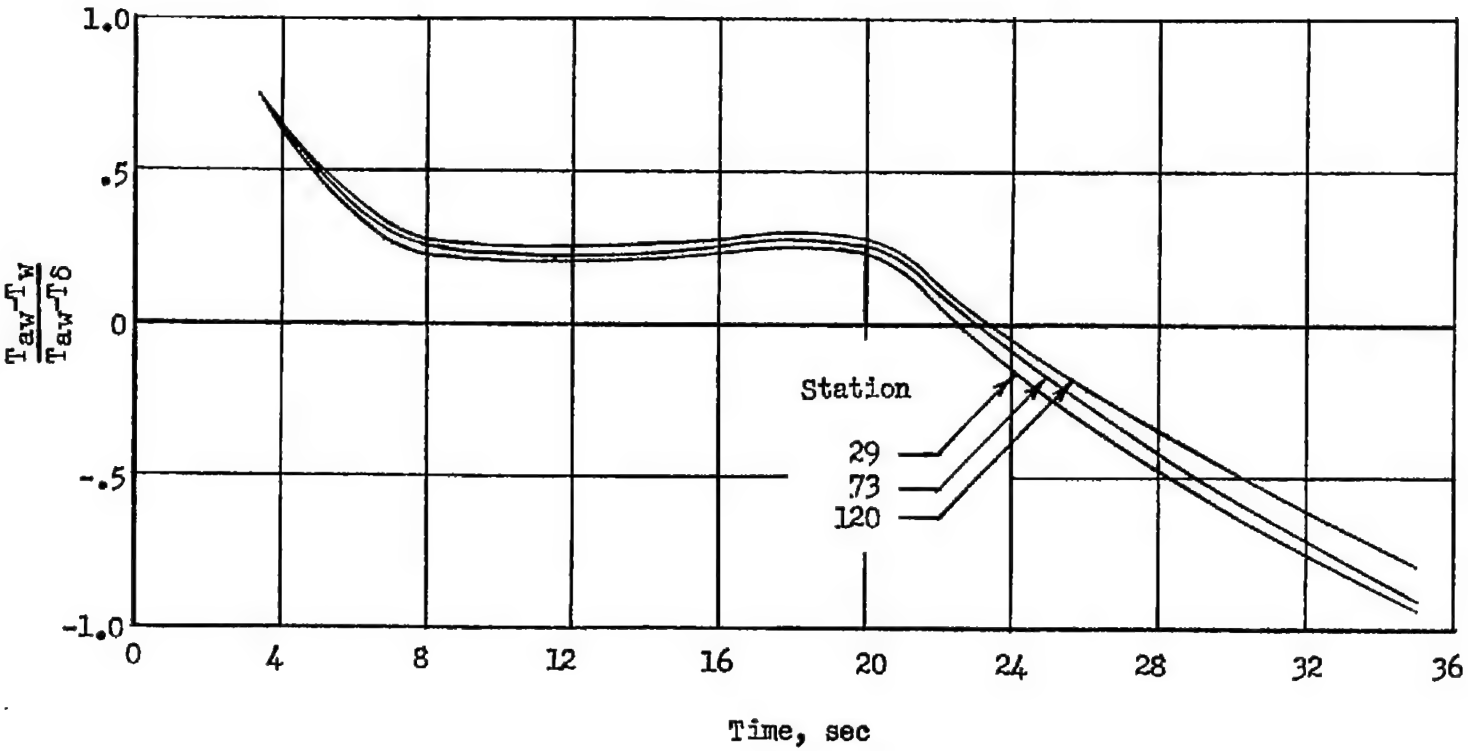

Figure 8.- Time history of the heating condition at the temperature measurement stations.

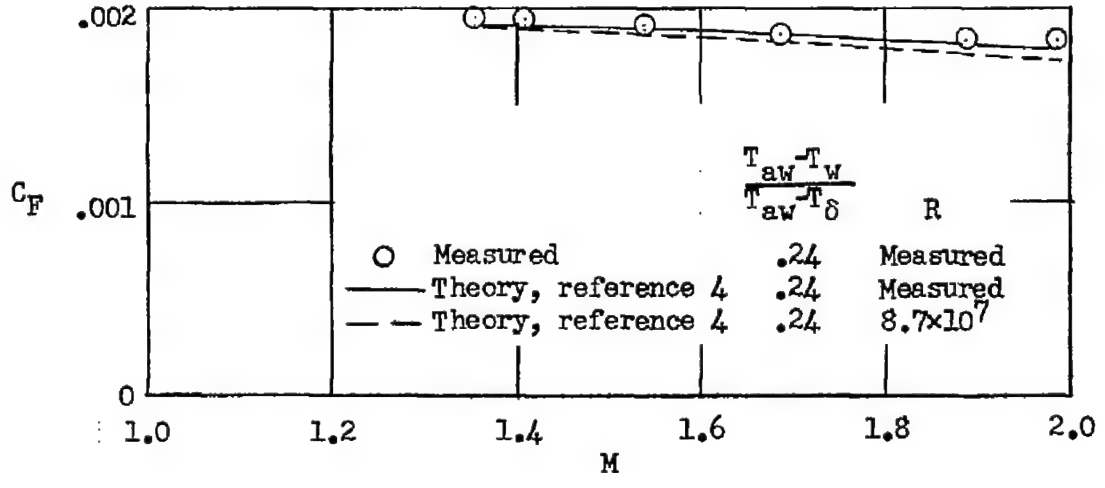

Figure 9.- Comparison of experimental average skin-friction coefficients measured during accelerating flight with theory of reference 4.

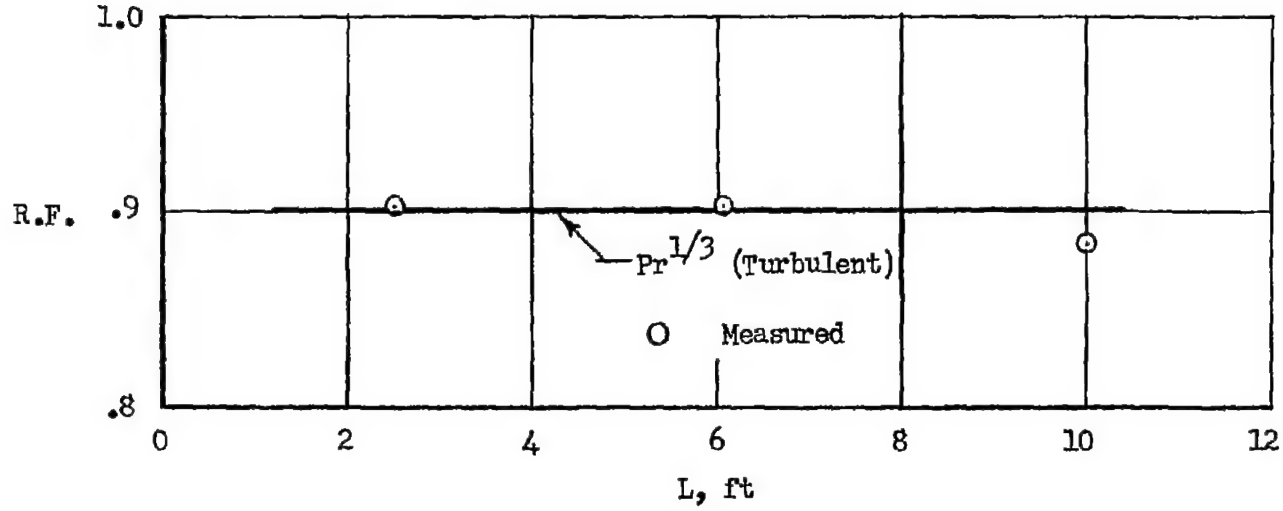

Figure 10.- Measured recovery factors at the three temperature-measurement locations. $M \approx 1.85$.

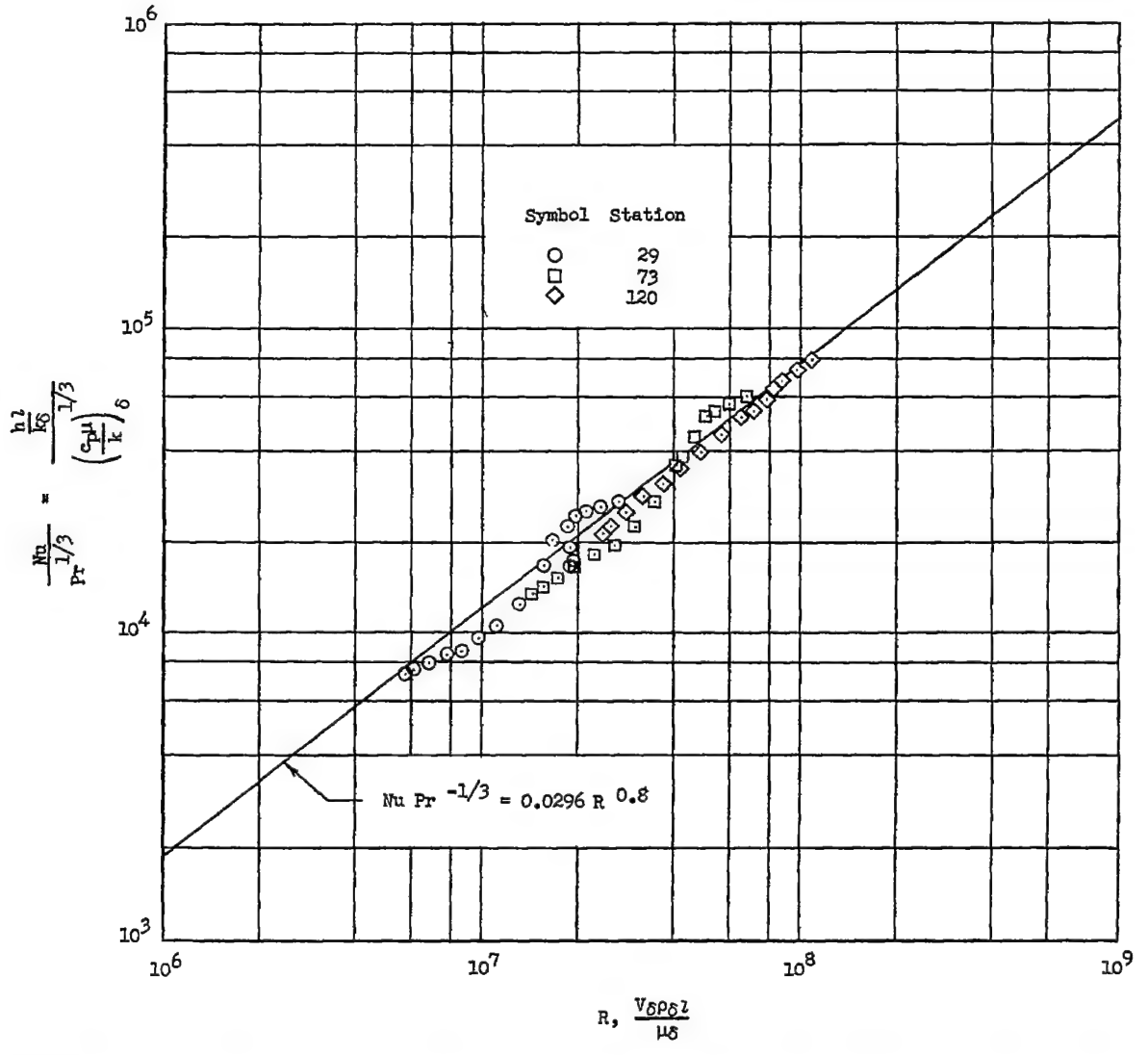

Figure 11.- Heat-transfer data with flow properties based on conditions just outside the boundary layer.

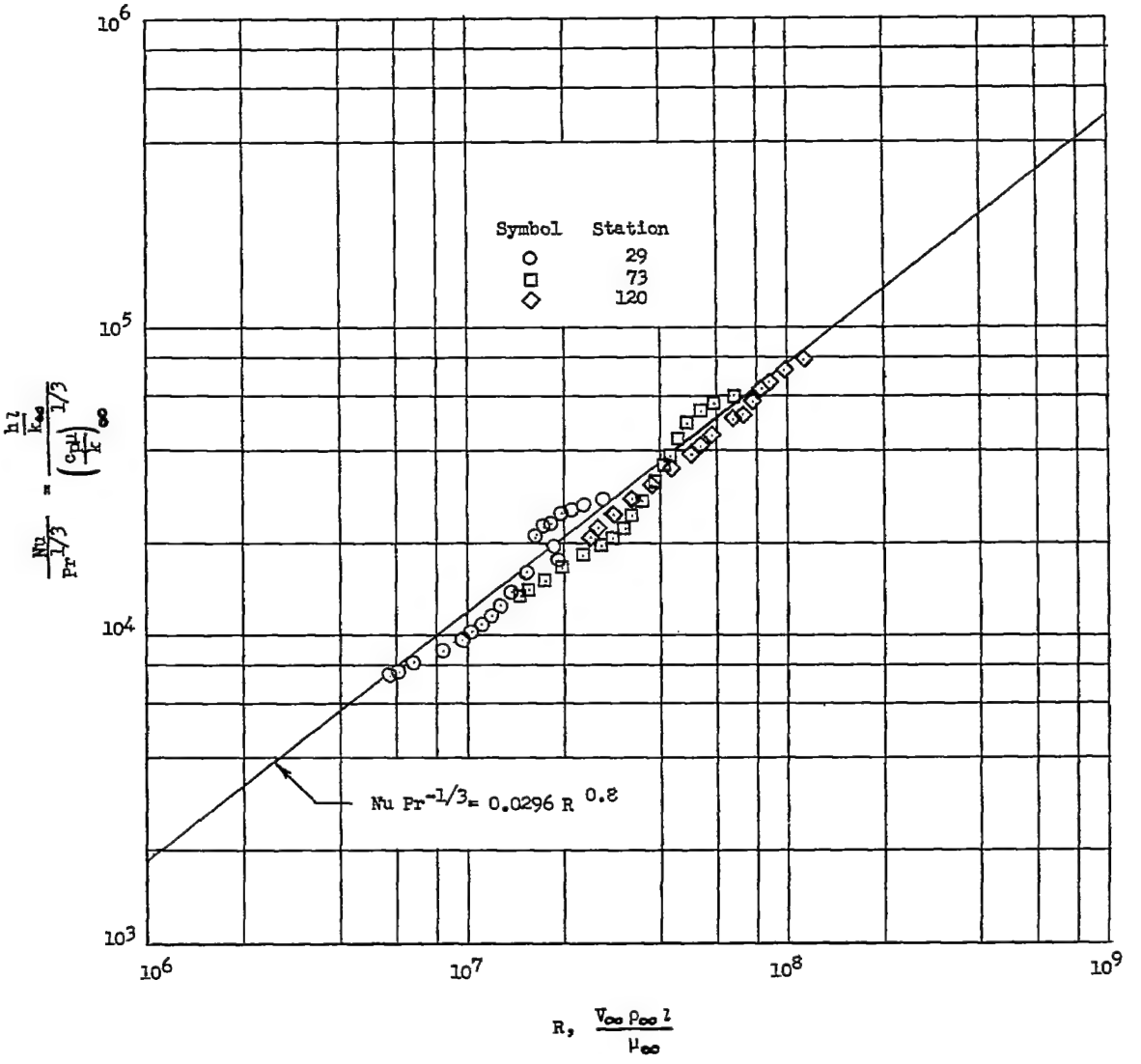

Figure 12.- Heat-transfer data with flow properties based on free-stream conditions.

[redacted]

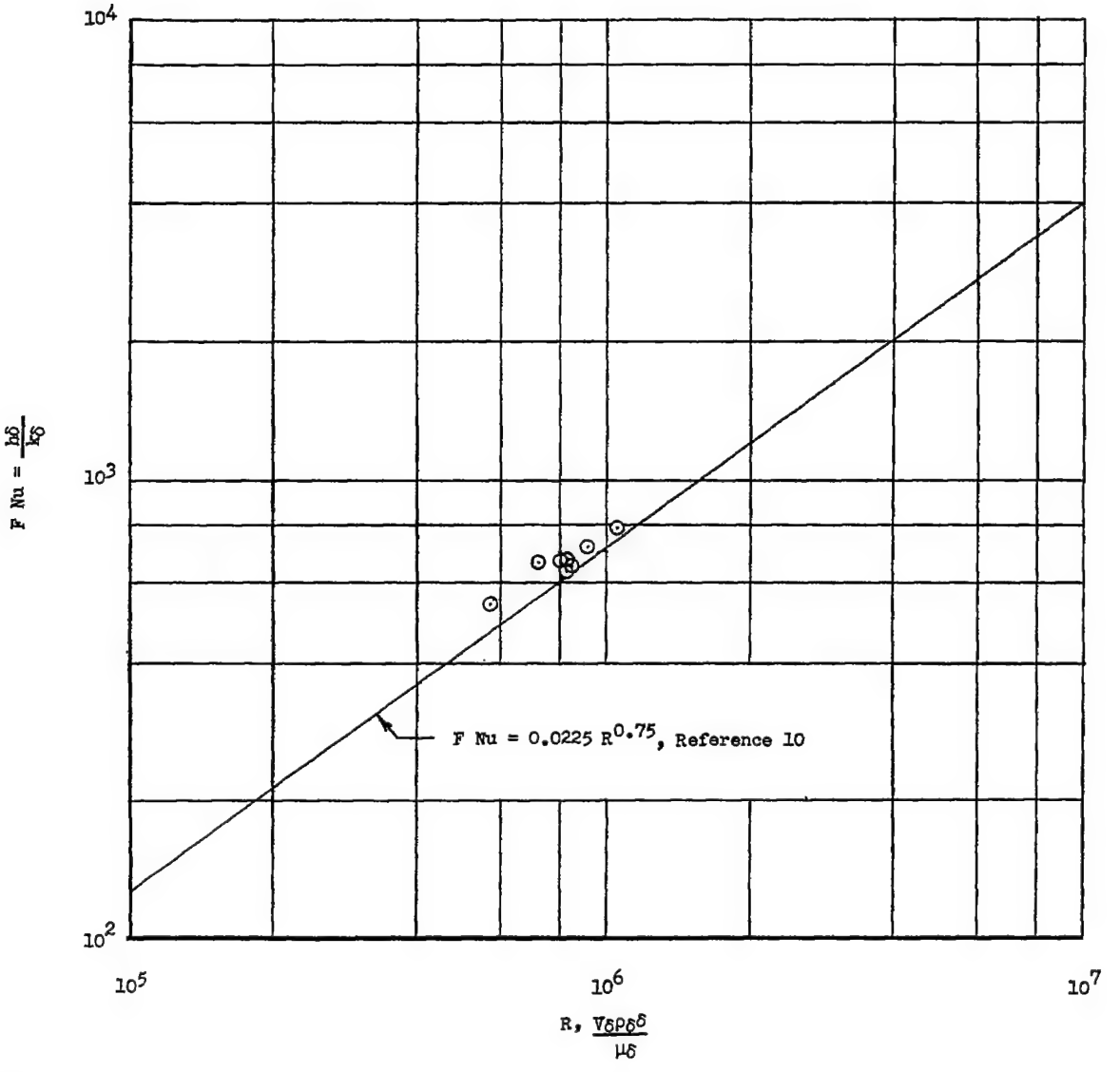

Figure 13.- Heat transfer at station 120 compared to Donaldson's theory.

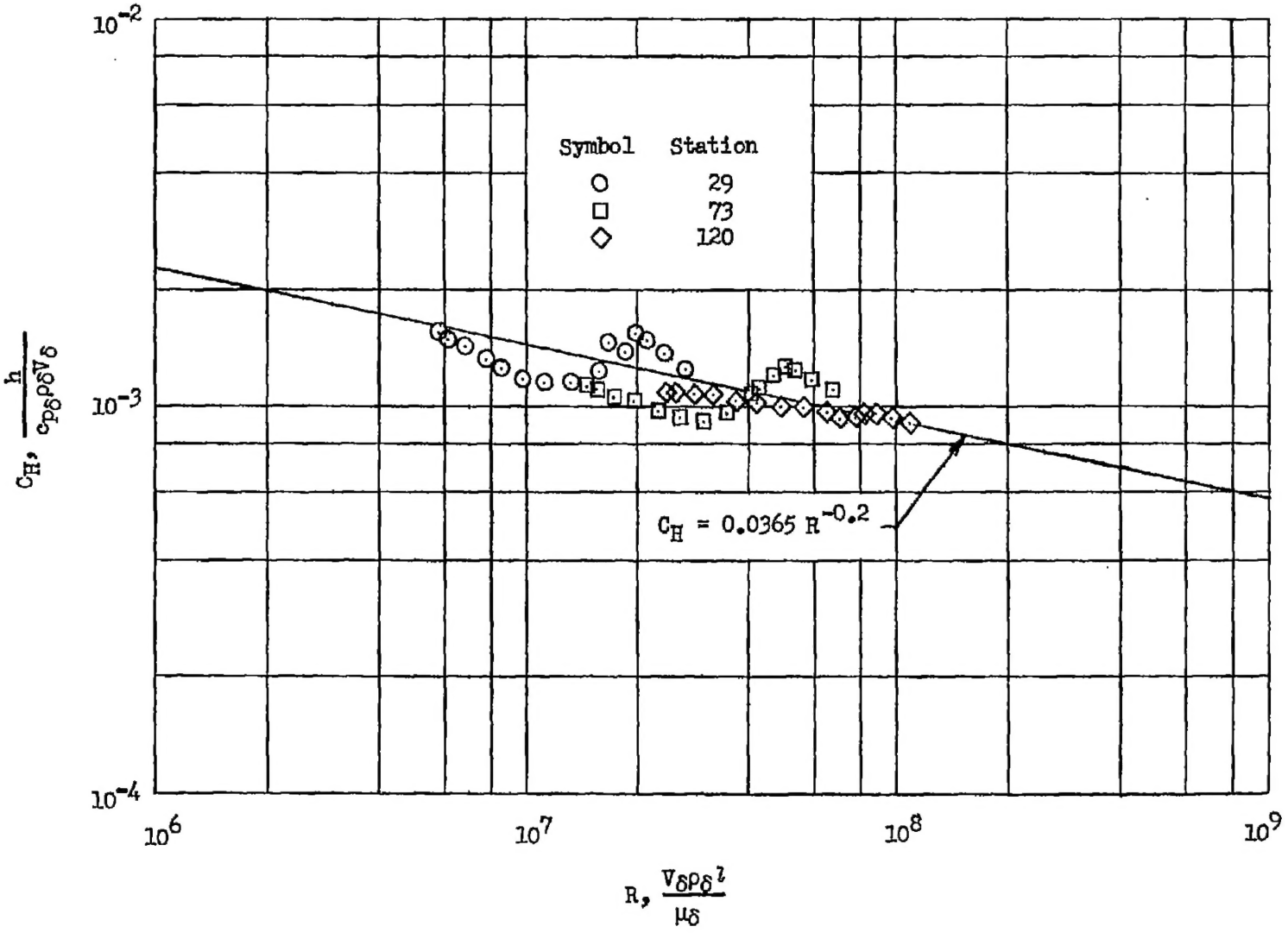

Figure 14.- Heat-transfer data with flow properties based on conditions just outside the boundary layer.

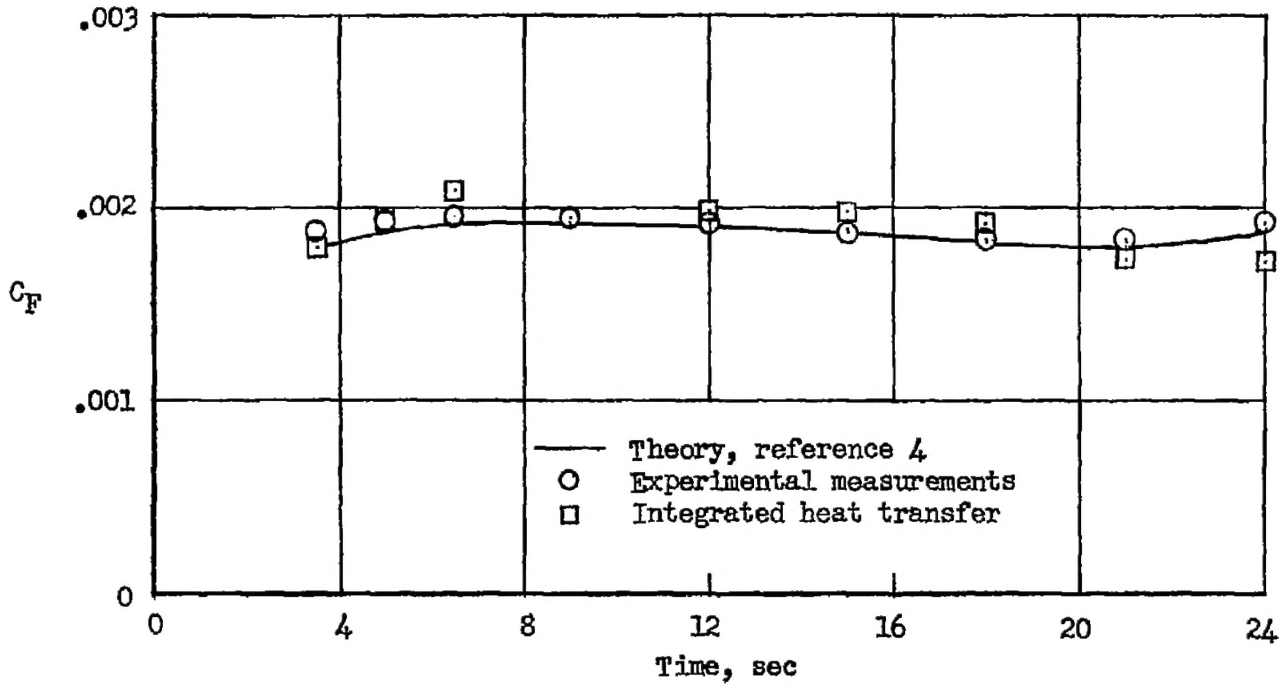

Figure 15.- Comparison of average skin-friction coefficient from integrated heat transfer with measured and theoretical values.

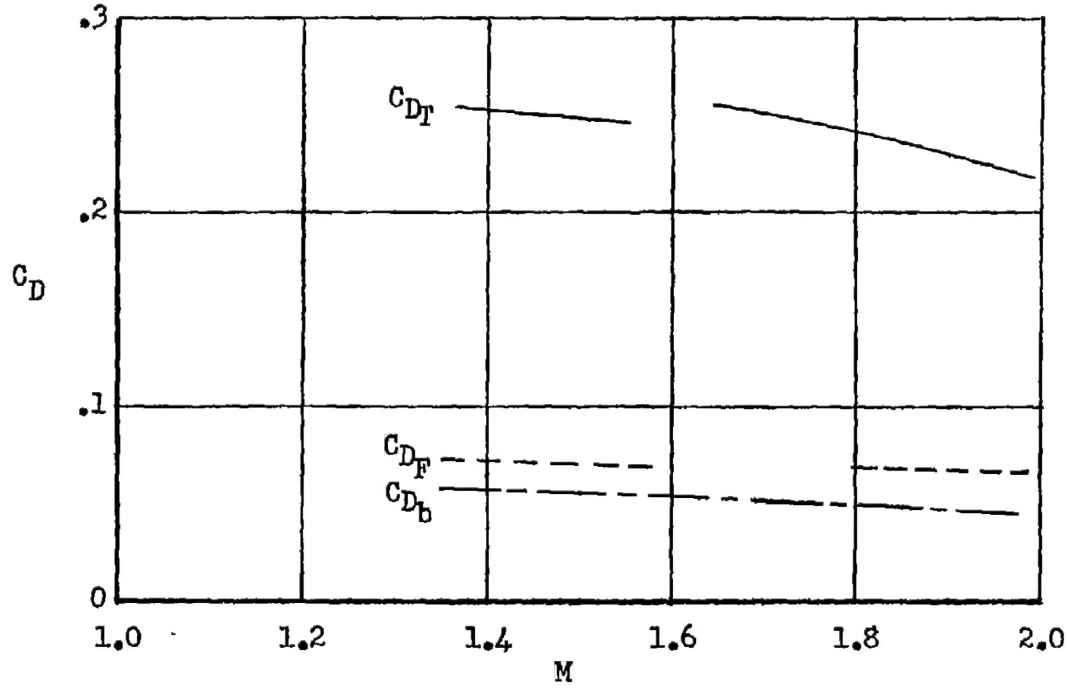

Figure 16.- Variation of total-drag, body-friction-drag, and base-drag coefficients, based on body frontal area, with Mach number obtained during decelerating flight.

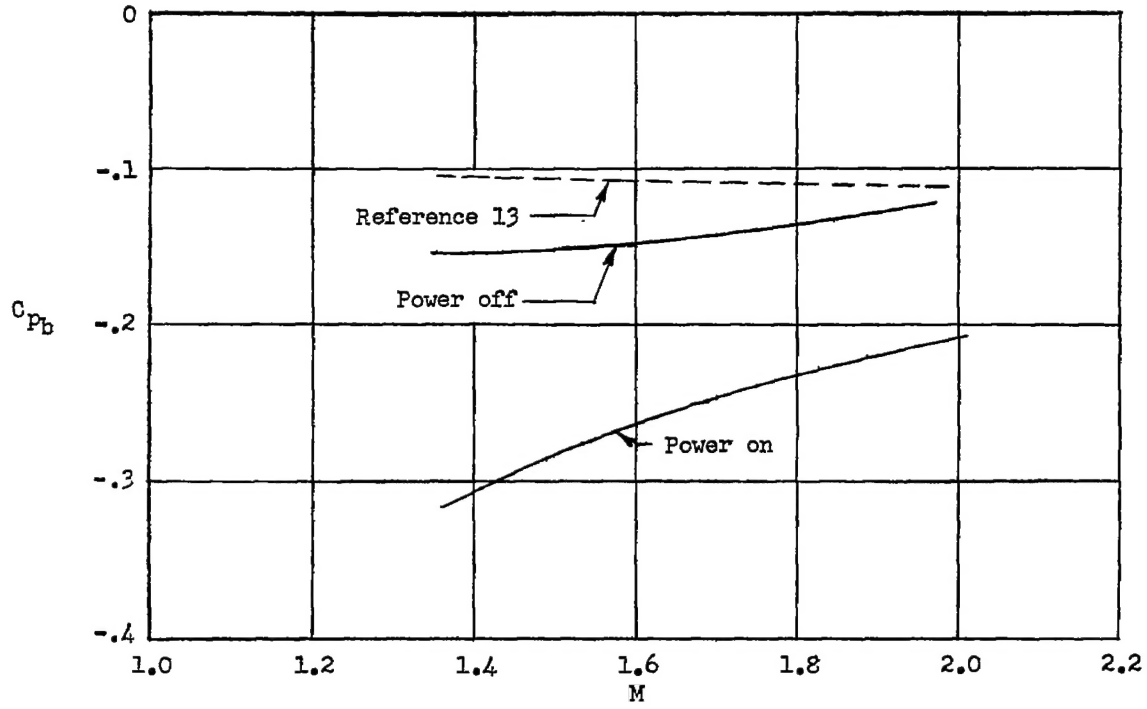

(a) Base-pressure coefficient.

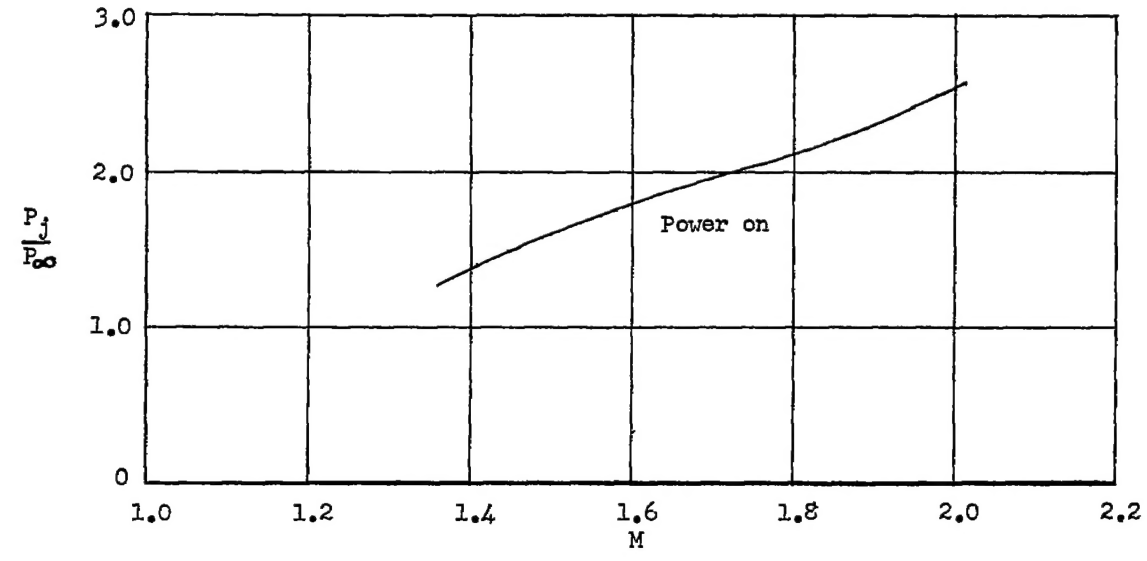

(b) Jet-exit pressure ratio.

Figure 17.- Variation of base-pressure coefficient and jet-exit pressure ratio with Mach number.

NACA-Langley - 6-17-54 - 350